

# A PI Sliding Mode Tracking Controller with application to a 3 DOF Direct-Drive Robot Manipulator

S. W. Nawawi, J. H. S. Osman and M. N. Ahmad

Lecturer, Faculty of Electrical Engineering, Universiti Teknologi Malaysia,  
81310 UTM Skudai, Malaysia. E-mail: [sophan@fke.utm.my](mailto:sophan@fke.utm.my)

## ABSTRACT

This paper deals with the tracking control of direct-drive (DD) robot manipulators. A robust Proportional-Integral (PI) sliding mode control law is derived for accurate tracking despite the highly non-linear and coupled dynamics. It is shown mathematically that the proposed controller is capable of withstanding the expected variations and uncertainties present in the system. The performance of the proposed control law is evaluated by means of computer simulation studies on a 3 DOF revolute DD robot manipulator actuated with BLDCM motors.

## 1. INTRODUCTION

The concept of direct-drive (DD) robot has been around for quite some time. It eliminates the problems associated with gear backlash and friction significantly. The construction is much stiffer, no wear and tear, and easy to maintain. In DD arm, the complex dynamics of the arm are directly reflected to the motor axes. Therefore, the varying inertia effect and the effects of the coupling and non-linear torques will have a substantial dynamical effect [1], [2]. Moreover, large inductance in typically used DD actuators, such as Brush-less DC Motors and Variable Reluctance Motors, will have a direct influence on the overall dynamics of the DD arm. In conventional SMC approaches, the starting point for the design procedure is through the transformation of the input distribution matrix  $B$  to some canonical form. The most commonly approach is to transform the system model into the *Reduced Form* or *Regular Form* whereby the matrix  $B$  is partitioned to the form  $[0 \ B_2]^T$  with  $B_2 \in R^{m \times m}$ . A variety of the SMC known as Integral Sliding Mode Control (ISMC) has surfaced in the literature [3]- [7]. In ISMC, the order of the motion equation in is equal to the order of the original system. It is not necessary to transform the original plant into a canonical form. Moreover, by using this approach, the robustness of the system can be guaranteed throughout the entire response of the system starting from the initial time instance.

## 2. PROBLEM FORMULATION

The integrated dynamic model of an  $N$  DOF DD revolute manipulator can be represented as [7];

$$\dot{X}(t) = A(X, \xi, t)X(t) + B(X, \xi, t)U(t) \quad (1)$$

$$X(t) = [X_1^T(t), X_2^T(t), \dots, X_N^T(t)]^T$$

$$X_i(t) = [\theta_i(t), \dot{\theta}_i(t), \ddot{\theta}_i(t)]^T$$

$$U(t) = [U_1(t), U_2(t), \dots, U_m(t)]^T$$

$$X_i(t) \in \mathcal{R}^3; i \in \mathfrak{I}$$

where  $\xi$  is a payload, and  $\theta$ ,  $\dot{\theta}$  and  $\ddot{\theta}$  are the joint angle, velocity and acceleration, respectively. The robot dynamics (1) can be represented as:

$$\dot{X}(t) = [A + \Delta A(X, \xi, t)]X(t) + [B + \Delta B(X, \xi, t)]U(t) \quad (2)$$

where  $A$  and  $B$  are nominal constant matrices, while  $\Delta A(X, \xi, t)$  and  $\Delta B(X, \xi, t)$  matrices are uncertainties.

Let  $X_d(t) \in \mathcal{R}^{3N}$  be the desired state trajectory:

$$\left. \begin{aligned} X_d(t) &= [X_{d1}^T(t), X_{d2}^T(t), \dots, X_{dN}^T(t)]^T \\ X_{di}(t) &= [\theta_{di}(t), \dot{\theta}_{di}(t), \ddot{\theta}_{di}(t)]^T \\ X_{di}(t) &\in \mathcal{R}^3; i \in \mathfrak{I} \end{aligned} \right\} \quad (3)$$

Define the tracking error,  $Z(t)$  as

$$Z(t) = X(t) - X_d(t) \quad (4)$$

in this study, it is assumed that there exist:

i) Continuous functions  $H(X, \xi, t) \in \mathcal{R}^{3 \times 3N}$  and

$E(X, \xi, t) \in \mathcal{R}^{3 \times 3N}$  such that for all  $X \in \mathcal{R}^{3N}$  and all  $t$ :

$$\Delta A(X, \xi, t) = BH(X, \xi, t); \quad \|H(X, \xi, t)\| \leq \alpha \quad (5)$$

$$\Delta B(X, \xi, t) = BE(X, \xi, t); \quad \|E(X, \xi, t)\| \leq \beta \quad (6)$$

ii) A Lebesgue function  $\Omega(t) \in \mathcal{R}^{m \times 1}$ , such that

$$\dot{X}_d(t) = AX_d(t) + B\Omega(t) \quad (7)$$

In view of (4), (5), (6) and (7), (2) can be written as

$$\begin{aligned} \dot{Z}(t) &= [A + BH(t)]Z(t) + BH(t)X_d(t) \\ &\quad - B\Omega(t) + [B + BE(t)]U(t) \end{aligned} \quad (8)$$

Define the PI sliding surface  $s(t) \in \mathcal{R}^{m \times 1}$  as

$$s(t) = CZ(t) - \int_0^t [CA + CBK]Z(\tau)d\tau \quad (9)$$

where  $C \in R^{m \times 3N}$  and  $K \in R^{m \times 3N}$  are constant matrices. The structure of matrix  $C$  is as follows:

$$C = \text{diag}[c_1 \ c_2 \ \dots \ c_{nj}] \quad (10)$$

The matrix  $C$  is also chosen such that  $CB \in R^{m \times m}$  is non-singular, while the matrix  $K$  satisfies

$$\lambda_{\max}(A + BK) < 0 \quad (11)$$

The condition in (11) guarantees that all desired pole are located in the left half plane to ensure stability. The control problem is to design a controller using (9) such that  $X(t)$  tracks  $X_d(t)$  accurately for all  $t$  in spite of the system uncertainties and non-linearities. In view of the error space, the tracking problem has become the problem of stabilizing the error system (8).

### 3. CONTROLLER DESIGN

The design task is divided into two parts; 1) To assure that the error dynamics must be asymptotically stable during the sliding mode, and 2) To design an SMC controller in such a way that whatever error the system has during the initial stage, the system must be directed towards the sliding surface during the reaching phase.

#### 3.1. System Dynamic During Sliding Mode

The equivalent control,  $U_{eq}(t)$  can be found by differentiating (10) and substituting (9) into it [7]:

$$U_{eq}(t) = -[I_n + E(t)]^{-1} \{ (H(t) - K)Z(t) - \Omega(t) + H(t)X_d(t) \} \quad (12)$$

Then the system dynamics during sliding mode can be determined by substituting (12) into (8):

$$\dot{Z}(t) = [A + BK]Z(t) \quad (13)$$

It is clear that the error dynamics during sliding mode are independent of the system uncertainties and couplings between the inputs, and, insensitive to the parameter variations, and may be determined through a proper selection of the desired closed loop poles locations.

#### 3.2. Controller Design

The manifold (9) is asymptotically stable in the large, if the following hitting condition is held [3]:

$$((s^T(t)\dot{s}(t)) / \|s(t)\|) < 0 \quad (14)$$

**Theorem:** The hitting condition (14) of the manifold (9) is satisfied if the control  $U(t)$  of system (2) is given by :

$$U(t) = -(CB)^{-1} [\gamma_1 \|Z(t)\| + \gamma_2 \|X_d(t)\| + \gamma_3 \|\Omega(t)\|] SGN(s(t)) + \Omega(t) \quad (15)$$

where

$$\gamma_1 > (\alpha \|CB\| + \|CBK\|) / (1 + \beta) \quad (16)$$

$$\gamma_2 > (\alpha \|CB\|) / (1 + \beta) \quad (17)$$

$$\gamma_3 > (\beta \|CB\|) / (1 + \beta) \quad (18)$$

**Proof:** See [5].

**Remark:** The above conditions guarantee not only that the hitting condition (14) is met, but it also assures that based on the Lyapunov theory, the system dynamics is stable in the large.

### 3.3. Input Chattering Elimination

In order to eliminate the control input chattering, the discontinuous function vector  $sgn(s(t))$  in (16) can be replaced by the following continuous function vector:

$$S_s(t) = \begin{bmatrix} \frac{s_1(t)}{|s_1(t)| + \delta_1} & \dots & \frac{s_i(t)}{|s_i(t)| + \delta_i} & \dots & \frac{s_m(t)}{|s_m(t)| + \delta_m} \end{bmatrix}^T \quad (20)$$

$i = 1, 2, \dots, m$

he continuous function vector (20) guarantees that the chattering problem encountered in the control input signal  $U(t)$  is removed. This will make the control more sensible from the practical point of view.

## 5. SIMULATION RESULT

The controller is applied to a 3 DOF revolute DD manipulator actuated by BLDCM motors as shown in Fig. 1. A complete set of non-linear dynamic equations of the robot model comprising the mechanical part of the robot and the actuator dynamics have been derived and used in the simulations. These equations were used in the simulation to represent a real DD robot manipulator without any approximation and simplification of the highly non-linear and coupled system. For the purposes of deriving the controller, the nominal matrices  $A$ ,  $B$ , as well as the bounds on the non-zero elements of the uncertainties matrices in (3) have been calculated based on the given range of the payload, joint angles and velocities.

The controller is required to track a reference cycloidal trajectory of the form:

$$\theta_{di}(t) = \begin{cases} \theta_i(0) + \frac{\Delta_i}{2\pi} \left[ \frac{2\pi t}{\tau} - \sin\left(\frac{2\pi t}{\tau}\right) \right], & 0 \leq t \leq \tau \\ \theta_i(\tau), & \tau \leq t \end{cases} \quad (21)$$

where  $\Delta_i = \theta_i(\tau) - \theta_i(0)$ ,  $i = 1, 2, 3$  and  $\tau$  is a final time.

Using (7) and (8), the bounds of  $H(X, \xi, t)$  and  $E(X, \xi, t)$  may be computed as follows:

$$\|H(X, \xi, t)\| \leq \alpha = 5.9874; \|E(X, \xi, t)\| \leq \beta = 0.6200 \quad (22)$$

Define the gain  $K$  as in (23) such that the closed-loop poles of the system are:

$$\begin{aligned} \text{Joint 1: } \lambda_1 &= \{-0.3, -0.31, -3.0\} \\ \text{Joint 2: } \lambda_2 &= \{-0.3, -0.31, -3.0\} \\ \text{Joint 3: } \lambda_3 &= \{-0.03, -0.031, -0.3\} \end{aligned} \quad (24)$$

Define the matrix  $C$  as:

$$C = \begin{bmatrix} 2 & 3 & 1 & 0 & 0 & 0 & 0 & 0 & 0 \\ 0 & 0 & 0 & 30 & 20 & 1 & 0 & 0 & 0 \\ 0 & 0 & 0 & 0 & 0 & 0 & 30 & 20 & 1 \end{bmatrix} \quad (25)$$

using (17) - (19), the controller parameter  $\gamma$  may be computed as follows:

$$\gamma_1 > 76.7962 ; \gamma_2 > 66.2157 ; \gamma_3 > 6.8566 \quad (26)$$

$$K = \begin{bmatrix} 0.01 & -0.59 & -0.26 & 0.07 & 1.27 & 0.07 & 0 & 0.67 & -0.01 \\ 0 & 1.65 & 0.09 & -2.99 & -0.21 & -0.21 & 0 & 0.06 & -0.11 \\ 0 & 0.42 & 0.02 & 0 & -0.24 & -0.06 & -0.07 & -0.08 & -0.06 \end{bmatrix}$$

(23)

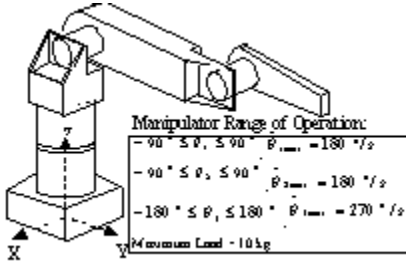


Fig. 1: A 3 DOF DD robot manipulator.

### 5.1. Effects of load variations

The simulation was carried out with the robot load fixed at its extremity i.e. no load and maximum load. Fig. 2, 3 and 4 show the tracking response of each joint. The tracking performances for both conditions are good for all joints, indicating that the controller is capable of withstanding the non-linearities and uncertainties present in the system.

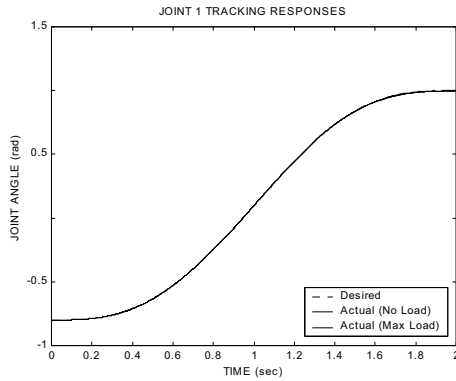


Fig. 2: Joint 1 tracking responses.

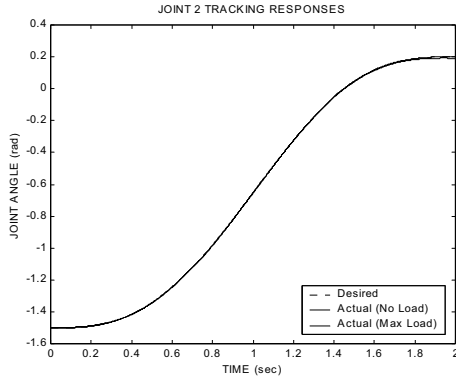


Fig. 3: Joint 2 tracking responses.

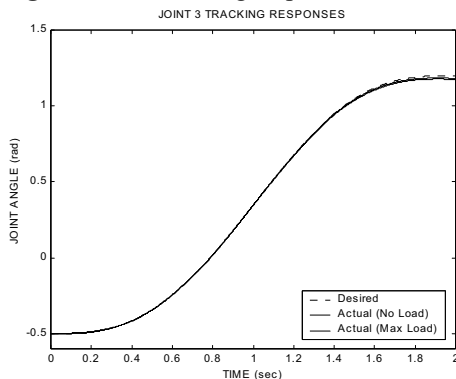


Fig. 4: Joint 3 tracking responses.

### 5.2. Effect of the PI Sliding Surface Constant

To study the influence of matrix  $C$  on the performance of the controller, the simulation was run again by a different set of the constant matrix  $C$  of (13). Throughout the simulations, a payload of 5 kg is attached to the end tip of the manipulator. The following desired poles location and the controller parameter  $\gamma$  has been used in the simulations:

$$\begin{aligned} \text{Joint 1: } & -3.0 \quad , \quad -3.1 \quad , \quad -30.0 \\ \text{Joint 2: } & -3.0 \quad , \quad -3.1 \quad , \quad -30.0 \end{aligned} \quad (27)$$

$$\begin{aligned} \text{Joint 3: } & -3.0 \quad , \quad -3.1 \quad , \quad -30.0 \\ \gamma_1 = 350 \quad ; \quad \gamma_2 = 300 \quad ; \quad \gamma_3 = 30 \end{aligned} \quad (28)$$

Three sets of the matrix  $C$  have been considered in the simulations:

$$C = \text{diag}[C_1 \quad C_2 \quad C_3] \quad (29)$$

where  $C_i = [c_{i1} \quad c_{i2} \quad c_{i3}] \quad ; \quad i = 1, 2, 3$

$$\text{Case 1: } C_i = [-3 \quad -3000 \quad 1] \quad (30)$$

$$\text{Case 2: } C_i = [-100 \quad 2000 \quad 1] \quad (31)$$

$$\text{Case 3: } C_i = [300 \quad 1000 \quad 1] \quad (32)$$

Figs. 5-7 illustrate the tracking performance for joints 1, 2 and 3, respectively, for all the above cases. It can be observed that Case 1 results in an over-damped response, while Case 2 and 3 produces under-damped responses, with all the trajectories enter the sliding region at about 3 seconds after the simulation start and remain there in for the rest of simulation time. These indicate that the shape of the trajectories during the reaching phase may be determined by the choice of the elements  $C_{i1}$  and  $C_{i2}$  of the constant matrix  $C_i$ .

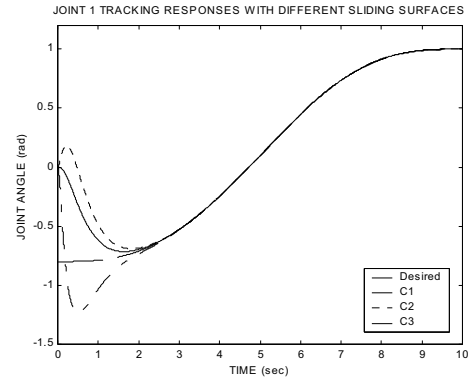


Fig. 5: Joint 1 tracking responses (different  $C$ ).

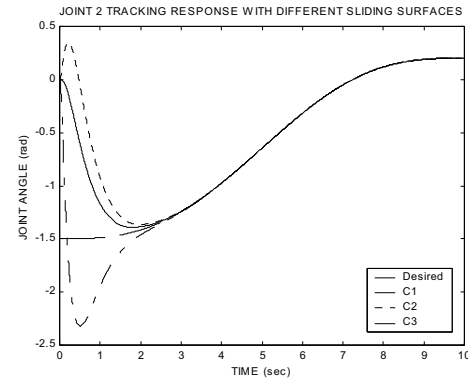


Fig. 6: Joint 2 tracking responses (different  $C$ ).

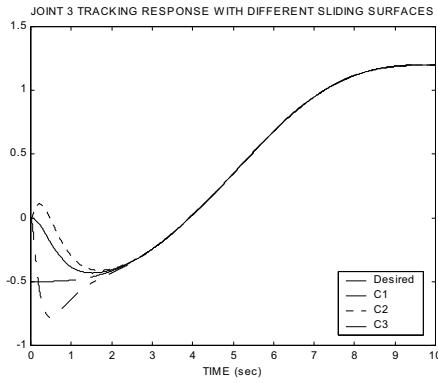


Fig. 7: Joint 3 tracking responses (different  $C$ ).

### 5.3. Control Input Chattering Suppression

The same sliding surface constant fixed as in *Case 1* are simulated again but with the discontinuous function vector  $SGN(s(t))$  replaced with a proper continuous functions vector  $S_\delta(t)$  described by (30). The simulation was performed with the continuous function constants  $\delta_i$ 's as shown in Table 1.

Table 1: Continuous Function Constants

JOINT	$\delta_i$		
	1	2	3
SET 1	200	100	60
SET 2	1000	550	250
SET 3	2000	800	600

The results are as shown in Fig. 8, 9 and 10. It can be seen that the chattering in the control input may be suppressed with a suitable choice of constant  $\delta_i$ . The value of  $\delta_i$  should be properly selected since too large values will only create unstable responses.

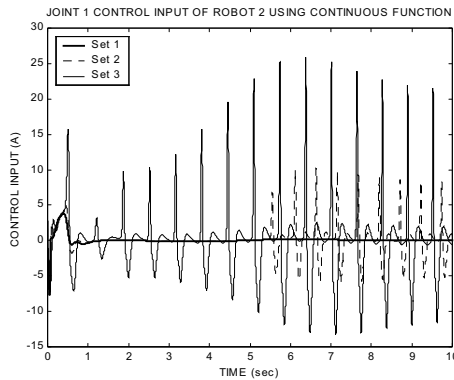


Fig. 8: Joint 1 control input.

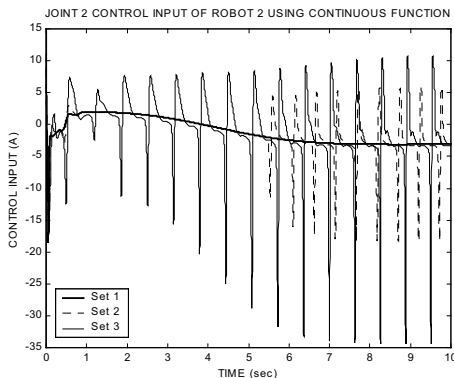


Fig. 9: Joint 2 control input.

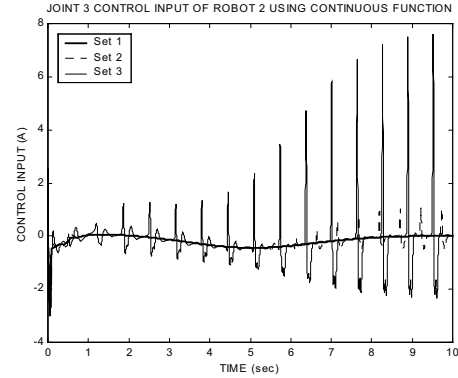


Fig. 10: Joint 3 control input.

## 6. CONCLUSION

A PI sliding mode tracking controller has been proposed for DD robot manipulators. The control law is formulated based on the assumption that the system uncertainties and non-linearities are bounded and these bounds are known. By mathematically it shown that the error dynamics during sliding mode is stable and can easily be shaped-up using the conventional pole-placement technique. The system actual trajectory is guaranteed to track accurately a desired trajectory despite the highly non-linear and coupled dynamics. Application to a three DOF revolute direct-drive robot manipulator confirms the effectiveness of the controller.

## 7. REFERENCES

- [1] H. Asada & K. Youcef-Toumi, *Direct-Drive Robots: Theory and Practice*(USA:MIT Press, 1987).
- [2] C. H. An, C. G. Atkeson & J.M. Hollerbach, *Model-Based Control of a Robot Manipulator* (USA: MIT Press, 1988)
- [3] J.-J. Yan, J.S.-H. Tsai & F.-C. Kung, Robust Decentralized Stabilization of Large-Scale Delay Systems Via Sliding Mode Control, *ASME Journal of Dynamic Systems, Measurement, and Control*, 119, 1997, 307-312.
- [4] K.-K. Shyu, F.-J. Lin, H.-J. Shieh & B.-S. Juang, Robust Variable Structure Speed Control for Induction Motor Drive, *IEEE Trans. On Aerospace and Electronic Systems*, 35(1), 1999, 215-223.
- [5] M.N. Ahmad, J.H.S. Osman & M.R.A. Ghani, Decentralized Tracking Controller Design using Proportional-Integral Sliding Mode Control", *Proc. IASTED Int. Conf. On Modelling, Identification, and Control (MIC 2002)*, Innsbruck, Austria, February 18-21, 2002, 368-373.
- [5] M.N. Ahmad, J.H.S. Osman & M.R.A. Ghani, Sliding Mode Control of a Robot Manipulator using Proportional-Integral Switching Surface, *Proc. IASTED Int. Conf. On Intelligent System and Control (ISC2002)*, Tsukuba, Japan, October 1-4, 2002, 186-191.
- [6] M. N. Ahmad and J. H. S. Osman, Application of Proportional-Integral Sliding Mode Tracking Controller to Robot Manipulators, *Proc. IEEE Conf. On Control Applications (CCA 2003)*, Istanbul, Turkey, June 23 - 25, 2003, pp.